SHAFT LOADS ON AZIMUTH PROPULSORS IN OBLIQUE FLOW AND WAVES

H Amini, and **S Steen**, NTNU, Norway
(DOI No: 10.3940/rina.ijme.2011.a1.199)

SUMMARY

A range of model experiments have been carried out in calm water and waves for an oil spill vessel model with twin tractor azimuth thrusters at different heading angles and advance coefficients in the large towing tank at the Marine Technology Centre in Trondheim, Norway. Propeller shaft bending loads have been measured using a shaft dynamometer capable of measuring all shaft side force and bending moment components as well as propeller torque and thrust. The results include the loads on the propeller shaft with and without the presence of a ship hull model at the same heading angles and advance velocities in order to study the wake influence from the ship hull on the hydrodynamic loads. Results show that the ship hull wake has a much stronger effect on the propeller loads when the propeller is azimuthed outward from the ship hull centreline than inward. Measurements from the experiments in waves are also presented for the same thruster model in a straight-line course for both the head and following sea states under different wave conditions. Larger bending loads are found in head sea conditions compared with the following sea conditions. Generally it is found that the shaft bending loads and lateral forces are quite large, which is important to consider in the mechanical design layout and for dimensioning of components.

NOMENCLATURE

A_w	Wave amplitude (mm)
$c_{0.7}$	Blade element chord at r = 0.7R
D_p	Propeller diameter (m)
f_z	Vertical force on propeller (N)
f_y	Horizontal force on propeller (N)
F_y^*	Total horizontal bearing force (N)
F_z^*	Total vertical bearing force (N)
F_r^*	Total radial bearing force (N)
J	Advance coefficient (-)
$K_T = \frac{T}{\rho n^2 D_p^4}$	Thrust coefficient (-)
$K_Q = \frac{Q}{\rho n^2 D_p^5}$	Torque coefficient (-)
$K_{fy} = \frac{f_y}{\rho n^2 D_p^4}$	Propeller horizontal force coefficient (-)
$K_{fz} = \frac{f_z}{\rho n^2 D_p^4}$	Propeller vertical force coefficient (-)
$K_{my} = \frac{m_y}{\rho n^2 D_p^5}$	Propeller horizontal moment coefficient (-)
$K_{mz} = \frac{m_z}{\rho n^2 D_p^5}$	Propeller vertical moment coefficient (-)
m_y	Propeller horizontal moment (N.m)
m_z	Propeller vertical moment (N.m)
n	Shaft rotational speed (rps)
Q	Propeller torque (N.m)
R_p	Propeller radius (mm)
T	Propeller thrust (N)
V_a	Advance velocity (m/s)
W_p	Propeller weight (N)
ν	Water cinematic viscose coefficient (N s $m^{-2)}$
δ	Propeller heading angle (deg)
$Fn = \frac{V_a}{\sqrt{gL}}$	Froude number (-)
$R_n = \left(nD_p C_{0.7} / \nu\right)\sqrt{(0.7\pi)^2}$	Reynolds number (-)

1. INTRODUCTION

Azimuth propulsors include both azimuthing thrusters and podded propulsors. Pods have an electric motor integrated into the unit, directly connected to the propeller shaft, while in azimuthing thrusters the propulsor powering machinery is located inside the ship hull, which drives the propeller through a system of shafting and bevel gearings [1]. Also, the size and shape of the housing of the azimuth thrusters and podded propulsors are usually different, with the pod housing being significantly larger than the typical azimuthing thruster housing.

It is the puller type of azimuth thruster that is addressed here. Note that although the focus here is on the puller type of azimuthing thrusters, the hydrodynamic loads related to oblique inflow are more or less the same for the pusher type azimuth and for podded propulsors. The

difference in hydrodynamic forces between pushing and pulling thrusters is extensively discussed in [2].

The main motivation for the study is the increasing popularity of azimuthing propulsors as main propulsion devices for a variety of ship types. In a study [3], problems with propeller shaft bearings have been identified as one of the most significant causes of mechanical failure. In addition to the bearing problems, there have also been some problems with bevel gears in the azimuth thrusters when used as main propulsion device. A detailed study of the bearing forces and moments due to the rotation of the propeller and the azimuthing of the pod unit is required to provide sufficient information for mechanical design engineering such as the development of optimum bearing systems. Therefore, it is important to know the hydrodynamic loads on the propeller shaft under all operating conditions. It has been found that the shaft side forces and bending moments in open water conditions at high oblique inflows and high advance velocities are large - so large that the shaft bearings experience three times larger load than when only the propeller weight is considered [2]. The hydrodynamic loads might be even higher when the thrusters work in the wake of a ship hull and in waves, which is the investigation of this paper. Further, the lack of knowledge about the hydrodynamic imposed propeller shaft forces has been identified for more than thirty years - for both conventional rudder-propeller and steerable propulsion systems [4]. The importance of the hydrodynamic imposed bending loads for the conventional rudder-propeller system has been addressed in [5].

One objective of this paper is to study the hull wake effect on the propeller performance and shaft bending loads in calm water at different thruster azimuth angles and ship velocities. There are a large number of publications on azimuth thrusters and podded propulsors, but they mainly focus on the propeller torque and thrust in calm water without the presence of the ship hull (see for instance [6], [7]). Islam and his colleagues at Memorial University have done a set of experiments to determine the hydrodynamic forces acting on podded propulsors. A difference from the study reported here is that Islam et.al. measured the six-degree of freedom forces on the entire thruster only, not on the propeller shaft as well. They have also investigated the effect of hub taper angle, pod-strut configuration and pod gap and pod–strut geometry on podded propulsor performance in open water [8], static and dynamic azimuthing conditions ([9], [10]). Pengfei Liu has performed a parallel development of numerical prediction of podded propulsor using a panel method ([11]). Investigation of the effect of the ship hull wake on the propeller performance has a long history in ship propulsion technology for the conventional rudder-propeller system [1]. However, it is quite new when it comes to azimuthing propulsors, since the wake experienced by an azimuthing propeller is strongly dependent on the azimuth angle. In the current study, propeller shaft loads in calm water in the presence of a ship hull have been measured at the same conditions as without the hull. The measurements without the hull are presented in detail in [2], with only comparisons shown here. By such a comparative study, one can get more insight into the ship hull wake's influence on the propeller performance and shaft side force and moment components.

In addition to oblique inflow, wave loading has been cited as one of the primary reasons for damage to propulsion thrusters [12]. It is also believed that wave loading is a contributing factor in fatigue damage to the aft tail shaft bearing in conventionally shafted propellers. These are found frequently and are very costly damages. For that reason, this study investigated the influence of waves and ship motion on the propeller performance and shaft bending loads. Some tests have been performed in waves to find the effect of waves and ship motion on propeller performance and the shaft side forces and bending moments. Ship motion actually causes another velocity component into the propeller disc in addition to the wave particle and hull wake velocities are superimposed on the ship motion effects and might change the propeller hydrodynamic loads significantly.

2. MODEL-HULL THRUSTER CONFIGURATION

A 5.4 meter long model of an oil spill vessel was fitted with two azimuth thrusters as the main propulsion device. The twin tractor azimuth thruster assembly was fitted to be aligned with the flow at the heaviest displacement. The port thruster was equipped with instrumentation to measure forces and moments in six degrees of freedom on the propeller shaft. On the starboard thruster, only propeller thrust and torque was measured. It is the measurements on the port thruster that is presented in this paper

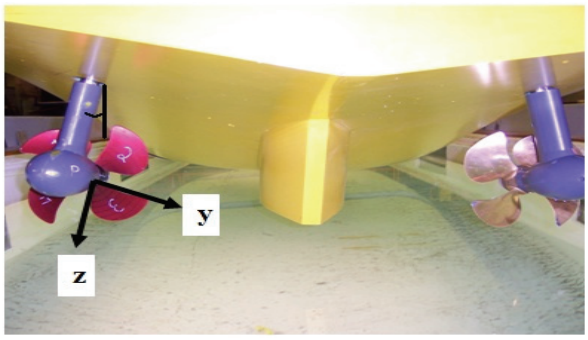

Figure 1: Coordinate system for local force measurements on the thrusters test set-up.

Descriptions of the measurement system for the propeller forces are found in ([2], [13]). The thruster configuration and local coordinate system for the local forces and moments on the propeller are presented in Figure 1. The main dimensions and form parameters are listed in Table 1 for the ship hull and in Table 2 for the propeller. The

gap between the propeller tip and under-side of the hull along a vertical line through the propeller centre was $0.25\,D_p$, in accordance with the classification society's recommendation.

The thruster strut was perpendicular to the hull bottom at the location of the thrusters, and therefore there was a tilt angle with respect to the water plane area both outwards (11° relative to the centre plane) and nose down (7.6°). There was no yaw angle (``toe out`` angle) from the centreline of the hull. The centre of the propeller was $1.306\,D_p$ below the waterline in order not to let the propeller blade tips come out of the water during severe wave conditions. The centres of the two propellers in the twin configuration were $3.026\,D_p$ apart. The thrusters' heading angle range was limited to $-40° \leq \delta \leq 40°$ in pulling mode, which was the same range as tested for thrusters without the ship hull. Torque and thrust were measured for both the port and starboard propeller, while the shaft side force and bending moment components were measured only for the port propeller.

Table 1: Model hull main dimension and form parameters

Length overall	L_{OA}	[m]	5.405
Length on designed waterline	L_{WL}	[m]	5.265
Length betw. perp.	L_{PP}	[m]	4.879
Breadth waterline	B_{WL}	[m]	1.266
Draught at $L_{PP}/2$	T	[m]	0.452
Draught at FP	T_{FP}	[m]	0.452
Draught at AP	T_{AP}	[m]	0.452
Volume displacement	∇	[m^3]	2.176
Prismatic coefficient	C_P	[-]	0.7846
Block coefficient	C_B	[-]	0.7792
Midship section coefficient	C_M	[-]	0.9931
Longitudinal C.B. from $L_{PP}/2$	LCB	[m]	-0.196
Wetted surface	S	[m^2]	9.547

Table 2: Propeller main specifications

Propeller diameter	250 mm
Hub diameter	60 mm
Design pitch ratio P/D_p	1.1
Skew	25 deg
Expanded blade area ratio	0.6

3. EXPERIMENTS

The shaft side force and bending moment components were measured in a reference frame rotating with the shaft, and then converted to a frame fixed with the thrusters by using the measured propeller angular position in Figure 1. The fixed reference frame is aligned with the thrusters as indicated in Figure 1, so that it is oriented at angles with the hull as described above. The propeller shaft rotational speed and pod azimuth angle were also measured. The positive thruster heading angle was defined clockwise when the thruster is viewed from above (inward to the ship hull centreline for the thruster measuring propeller side forces).

Since the shaft side force and bending moment are converted in the coordinate system fixed with the shaft, the magnitude of the radial force and moment (resultant force and moment) could be obtained. In addition to the tests in calm-water, the propeller and shaft loads were also measured in regular waves in different sea states to investigate the effect of the hull motion (mostly pitching) on the periodic propeller loads. Measurements were made only in head and following sea conditions in a straight-line course.

3.1 EXPERIMENTAL PROCEDURE IN CALM WATER

The tests were carried out with the two azimuth thrusters at the same azimuth angle. The tests were repeated for different conditions i.e. different azimuth angles and different advance velocities. In order to cover a range of advance coefficient the carriage velocity was varied in the towing tank. To avoid the complication of autopilot control, the ship was restrained from the swaying and yawing motion by using a system of cables and a transverse beam, shown in Figure 2.

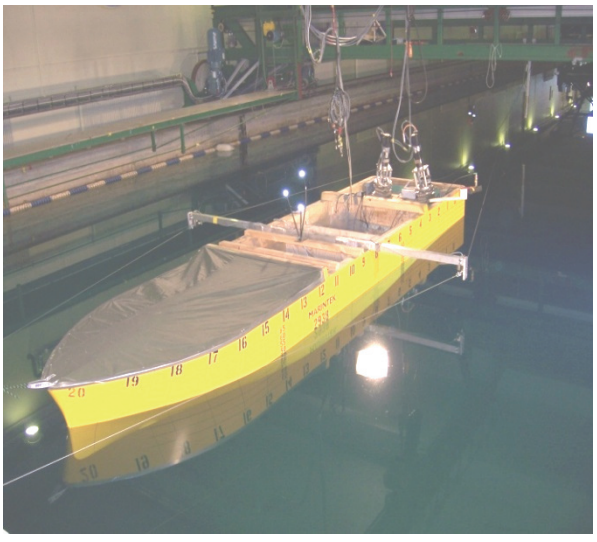

Figure 2: Test set-up for the experiment using a system of cables and bar to keep the model fixed in yaw.

This connection system restrained the model in surge, and thereby controlled the velocity of the model. The loading on the propeller shaft might be different for the thrusters at negative and positive heading angles. Hence, data was measured over the range $-40° \leq \delta \leq 40°$. The

tests were performed with model advance speeds corresponding to Froude numbers in the range $0.0434 \leq F_n \leq 0.217$ and its associated propeller advance coefficient range $0.2 \leq J \leq 1$. The propeller's rotational velocity was kept at 6 rps for the duration of the experiment in order to avoid propeller ventilation, and ensure similar conditions as those for tests performed without the hull [2].

The range of the propeller blade's Reynolds number was 0.32×10^6 - 0.35×10^6 (Rn). Viscous scale effects typically exist for Reynolds numbers below 0.2×10^6. The range of the Reynolds number for the strut part of the body was from $2.58\times10^4 - 1.29\times10^5 (R_n = \frac{VL}{v})$. In a previous study of the thruster in open water [2], tests were performed at both 6 and 12 rps at low azimuth angles, and the differences in K_T and K_Q between the two propeller speeds were within 6%, something that confirms that the relatively low Reynolds numbers in these tests still can be expected to provide reliable results. The nominal Reynolds number range corresponding to the model speeds tested was from 1.496×10^6 - 7.48×10^6. For hydrodynamic bodies, a Reynolds number of 5×10^6 is usually considered adequate for model results to be representative of the full scale [8]. The attachment of boundary layer turbulence stimulators to the hull and pods would be expected to create effective Reynolds numbers that were higher. The hull model was equipped with a 1 mm diameter cotton tread at station 19½ as a turbulence stimulator, while there was no turbulence stimulation at the thruster body. However, since most of the thrusters' body is inside the propeller slipstream, the flow is also expected to be turbulent without extra turbulence stimulation. Thus, the results are expected to be representative of full-scale performance.

3.2 DISCUSSION OF RESULTS IN CALM WATER

The time average of all the forces and moments on the propeller behind the ship hull are compared with open water tests in the pulling condition at the same heading angles and advance velocities, so that the ship hull wake effect on the propeller performance and shaft loads can be investigated.

Figure 3 and Figure 4 compare the propeller torque and thrust between open water conditions and behind the hull. At a higher oblique inflow angle, the effective advance velocity (axial component of oblique inflow) is lower (the effective advance coefficient Je=J*cosθ, where θ is the heading angle), leading to higher torque and thrust than with lower oblique inflow angles. In other words, as the propeller is subjected to a larger heading angle, the propeller blades experience higher angle of attack leading to larger loads.

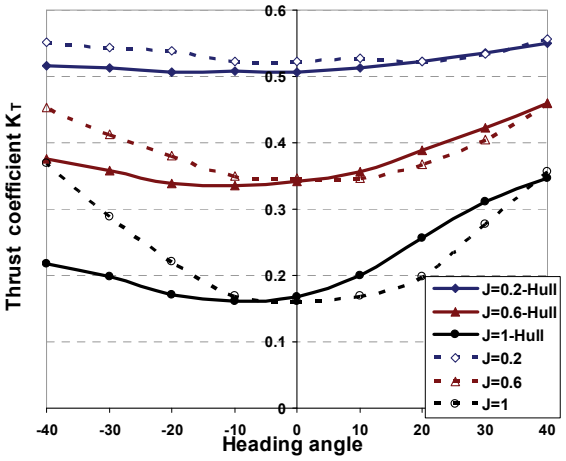

Figure 3: Comparison of the thrust coefficient between open water and behind the hull conditions

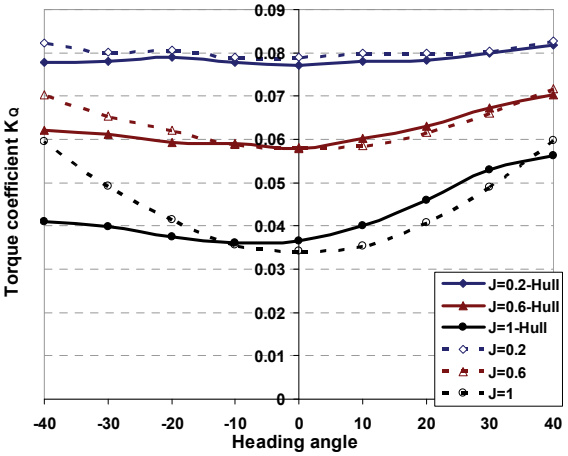

Figure 4: Comparison of the propeller torque coefficient between open water condition and behind the hull

The torque and thrust are asymmetric with respect to positive and negative heading angles when the propeller works behind the ship model, whereas this is not the case in open water conditions. For the port thruster studied here, negative heading angle means that the thruster points outwards. In the stern area of the ship, the flow is generally directed inwards (and upwards), so that when the thruster points outwards it is oriented (partly) in the direction of the incoming flow. Thus, the effective heading angle is less than the nominal azimuth angle.

In positive heading angles the propeller gives slightly higher thrust and torque behind the ship than open water conditions, since in this case the in-plane velocity from the hull wake and from the azimuth angle are adding, not cancelling as for negative heading angles. The in-plane velocity from the ship hull wake seems to be weaker in positive heading angles (inward toward the ship hull centre) than in negative heading angles. This is not unexpected, since the propeller position changes with heading angle, so a change in hull wake field at the propeller can be expected. In positive heading angles, when the propeller is moved closer to the centreline, the axial wake component is expected to increase, i.e. the

advance ratio decreases, something that leads to increased thrust and torque.

Oblique inflow, gives rise to two flow components acting at the propeller plane. The first component is parallel to the shaft and the second is perpendicular to the shaft. In oblique inflow, due to the different sense of in-plane velocity component (perpendicular to the shaft) in the tangential direction to the propeller experienced by different parts of the propeller leads to a difference in the thrust between different sides causing a net hydrodynamic bending moment. In other words, in oblique inflow the perpendicular velocity component presents an asymmetry when viewed in terms of propeller relative velocities, since on one side of the propeller disc the perpendicular velocity component is additive to the propeller rotational velocity whilst on the other side it is subtractive. This gives rise to a differential loading of the blades as they rotate around the propeller disc, which causes a thrust eccentricity and side force components. Therefore, it is worth mentioning that it is the tangential component of inflow velocity to the propeller caused by the overall in-plane velocity, which is important for the side forces and bending moments. Even though the radial component of inflow gets a similar contribution from the in-plane velocity it is believed to be of less importance for the side forces and bending moments.

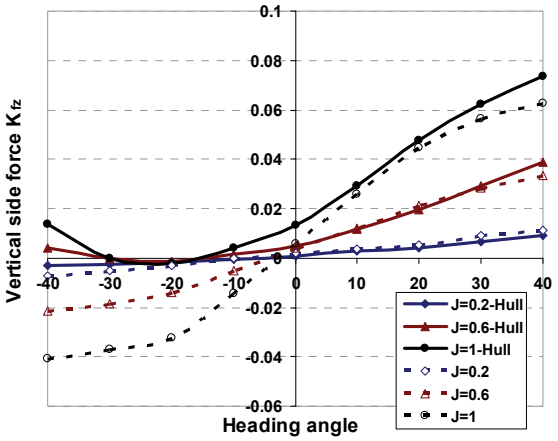

Figure 5: Comparison of the vertical component of the side force coefficient between open water condition and behind the hull

Figure 5 and Figure 6 show the vertical component of the side force and bending moment for the thruster propeller in open water and behind conditions. The side forces and bending moments in negative heading angles are much higher for the open water condition than for the behind condition due to a smaller effective heading angle, similar to torque and thrust results. In positive heading angles, the differences are smaller, with the forces in the behind condition being slightly larger than in open water.

Figure 7 and Figure 8 show the comparison between open water tests results and results for the thruster in behind condition for the horizontal component of the side force and bending moment. The horizontal force increases with the increase in heading angle and advance coefficient. The larger horizontal force at a higher heading angle with the same advance coefficient is believed to be due to the stronger in-plane velocity component to the propeller disc compared to the lower heading angle. The increase in horizontal force with increasing advance coefficient is expected because the induced axial velocity is large compared to the incoming flow velocity at low advance coefficients, so the effective heading angle is significantly less than the geometric one.

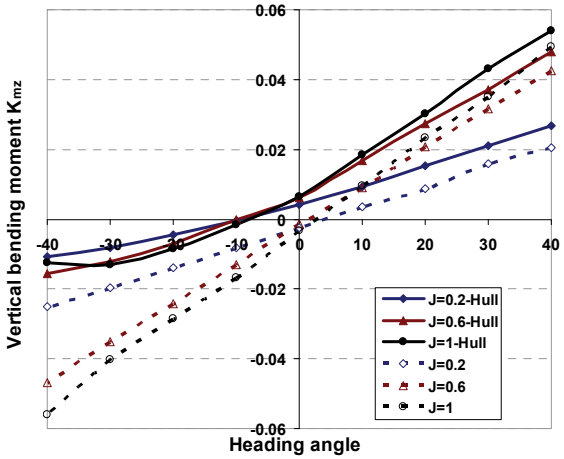

Figure 6: Comparison of the vertical component of bending moment coefficient between open water condition and behind the hull.

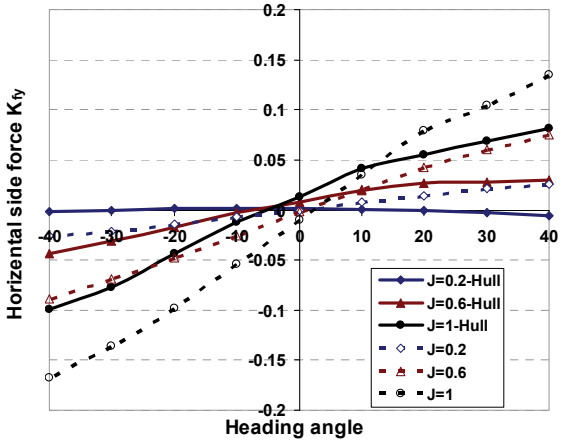

Figure 7: Comparison of the horizontal component of the side force coefficient between open water condition and behind the hull

Again, the side force and bending moment components in the horizontal direction are higher for open water than in the behind condition for negative heading angles. The explanation is believed to be the same as for the vertical force and bending moment (see above). In purely oblique inflow, typically due to steering, without considering any wake from the thrusters' body and ship

hull, the horizontal components of the side force and bending moment are a consequence of non-uniform inflow in the tangential direction to the propeller disc due to in-plane velocity to the propeller disc from the oblique inflow. Higher oblique inflow gives bigger side force and bending moment.

Contrary to other components, in positive heading angles, the horizontal side force and bending moment are slightly higher for the open water condition than when the propeller works behind the hull. The reason for this relationship is the higher arm of the eccentric thrust in the z coordinate system in the open water condition, leading to larger bending moment in the y direction (see Figure 9), even though the thrust in the behind condition is slightly higher than in open water conditions (see Figure 3).

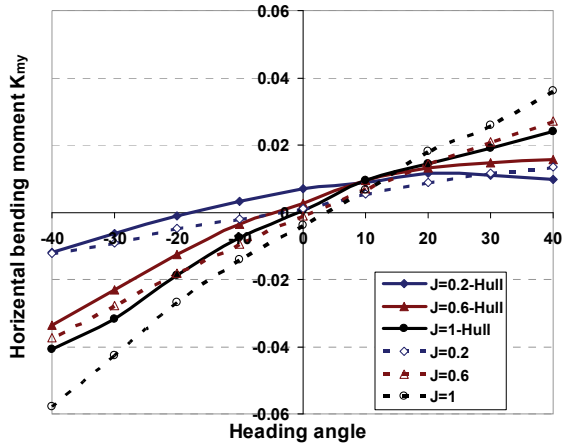

Figure 8: Comparison of the horizontal component of the bending moment coefficient between open water condition and behind the hull

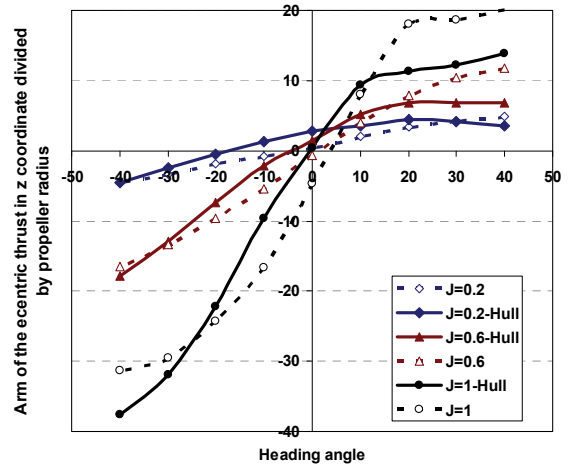

Figure 9: Centre of the eccentric thrust in the propeller disc in z coordinate system as a percentage of the propeller radius

It seems that the tangential wake component is not dominant in positive heading angles, and therefore not only the tangential wake but also the axial wake component influences these components of the side force and bending moment. When the axial wake varies over the propeller disc it should induce the bending moment and lateral force. The axial wake into the propeller disc depends on the thruster azimuth angle, with the axial wake being larger and closer to the hull (inner and upper part of propeller disc). So, the location of the centre of the propeller disc relative to the hull in different azimuth angles is considered to be important. The location of the propeller centre in different azimuth angles is shown in Figure 10. It is worth mentioning that it is common to decompose the total wake into three components:

- Potential wake without considering the steady wave pattern made by the hull
- Viscous wake due to the viscous nature of the boundary layer
- Wake component due to action of the waves set by the hull (steady wave pattern)

It is believed that the viscous wake is the main contribution of the total wake (80-90% of total wake) [14]. It is known that a single screw propeller mainly operates within the viscous wake where the wake effect is important, while a twin screw propeller to a larger extent operates outside of the viscous wake (mostly in the potential wake) so the viscous effect is therefore less important twin propeller arrangements. Thus, for a ship with twin azimuth thrusters there will be a more significant potential wake effect experienced by the propeller when the thruster is azimuthed outward from the ship centreline, while when the thruster is azimuthed inward the viscous wake is dominating. It is possible that when turning the thruster towards the hull, there will be larger differences in axial wake over the propeller disk than when the thruster is turned outwards, leading to a larger change in the arm of the off-axis thrust. The effect of axial wake is observed in the horizontal component of force and moment in positive heading angles such that propeller gives less horizontal bending moment and side force in behind conditions than in open water conditions.

The effect of only the ship hull wake in all the components of force and moment is seen at zero heading angles from the comparison between open water condition results and when propeller works behind the ship hull. However, it should be noted that the wake at the propeller changes with heading angle, since a change of heading changes the propeller position relative to the hull. More detailed knowledge of wake velocities in both axial and tangential directions is necessary to see the contribution of both components of the wake hull in relation to the change of results.

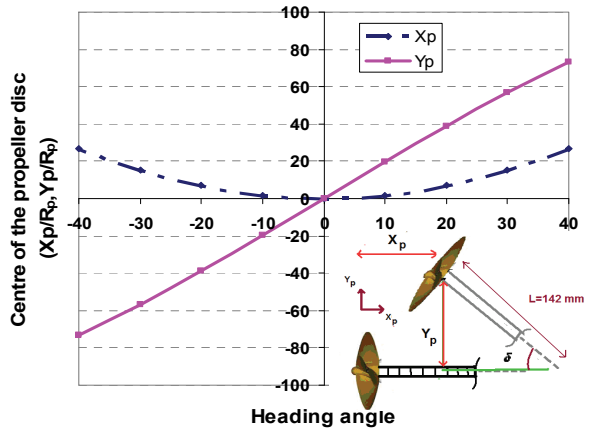

Figure 10: Propeller disc centre relative to the propeller centre at zero heading angles in different propeller azimuth positions (Values are presented as a percentage of the propeller radius)

3.3 EXPERIMENTAL PROCEDURE IN WAVES

The tests in regular waves were carried out using the same propeller shaft rotational speeds and advance velocities as in calm-water, corresponding to the $0.0434 \leq F_n \leq 0.217$ Froude number range and its associated $0.2 \leq J \leq 1$ propeller advance coefficient range. The propeller heading angle was held at zero degrees for all tests in waves. The model was free to heave and pitch in waves. The range of the propeller blade Reynolds numbers was $0.32 \times 10^6 - 0.35 \times 10^6$. The model held course at 0 and 180^o into the waves in all wave conditions. The influence of ship motion on the propeller loads was investigated by carrying out the experiments at different wave amplitudes and frequencies. The applied regular waves are shown in Table 3. Waves were chosen in order to avoid the propeller blade tips coming out of the water during the experiments. Also, for this reason, the experiments were carried out at the largest model draft.

Table 3: The list of regular waves selected for the experiments in wave conditions

Name	T (s)	Height (mm)	Wave Heading
HS-2s-225mm	2	225	Head
HS-2s-170mm	2	170	Head
HS-2s-160mm	2	160	Head
FS-2s-160mm	2	160	Following
FS-2s-200mm	2	200	Following

In addition, during the model tests, the ship model speed, propeller speed, incoming wave elevation, ship motion and acceleration in heave, and the model resistance were also measured.

3.4 DISCUSSION OF RESULTS IN WAVES

A typical record of propeller load fluctuation is shown in Figure 11.

All the presented results in waves, except Figure 11, are filtered with a low-pass filter with cut-off frequency of 5Hz. Note that the frequency of the higher frequency oscillations, seen in Figure 11, is that of the blade. The low frequency corresponds to the wave encounter frequency. The low-pass filter removes the propeller blade frequency variations, but retains the wave encounter frequency response.

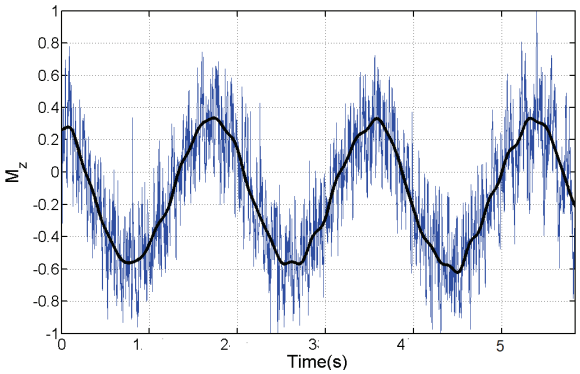

Figure 11: Typical record of loads on the propeller fluctuation in waves

A sample of variation of propeller force and moment amplitudes components is given in Figure 12. The periodic loads are presented versus time.

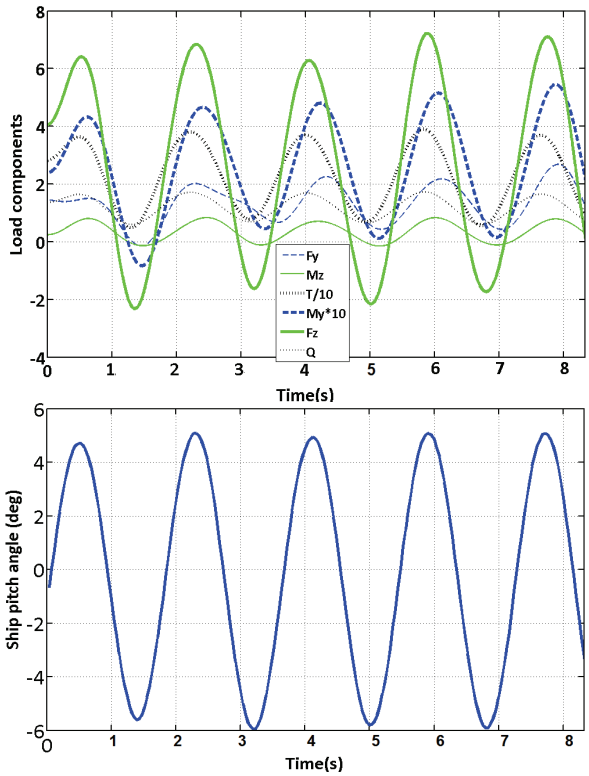

Figure 12: Variation of propeller loads for different components.

Generally, the peaks in loads are found when the hull pitch passes through the maximum values (stern-down

and stern-up), and the minimum load is near the zero pitch value (zero pitch angle). It is noted that there is a small phase difference in maximum loads between different components.

It is worth noting that the load fluctuation is not only the consequence of ship motion. The non-uniform inflow into the propeller disc due to the induced wave particle velocity also leads to variation in the propeller loads in a periodic manner.

When a propeller works in waves without presence of ship hull, and being fixed vertically, the propeller loads change periodically in correspondence with the wave elevation at the position of the propeller. This is discussed extensively in [2], in which the experiments done in open water conditions in waves without the ship hull are reported. The peaks of the propeller torque and thrust are observed when the propeller is located at X=0, L/2, and L relative to the wave (see Figure 13). In other words, the propeller gives the maximum torque and thrust when the averaged velocity induced by wave particles in the propeller disc is purely axial and in the opposite direction of the incoming flow leading to the lowest effective advance coefficient (X=L/2). The propeller gives the minimum torque and thrust at X=0 and X=L; because in these points the purely axial velocity induced by wave particles is in the same direction as incoming flow leading to the highest effective advance coefficient.

Generally, waves cause a non-uniform inflow into the propeller which causes bending moments and side forces on the propeller shaft. The peaks in side forces and bending moments are observed at times corresponding to X=L/4, X=3L/4 when there is purely strong in-plane velocity into the propeller disc generated by the wave particles as in the same way as for oblique inflow leads (see for instance the horizontal bending moment form the experiment in Figure 14) .

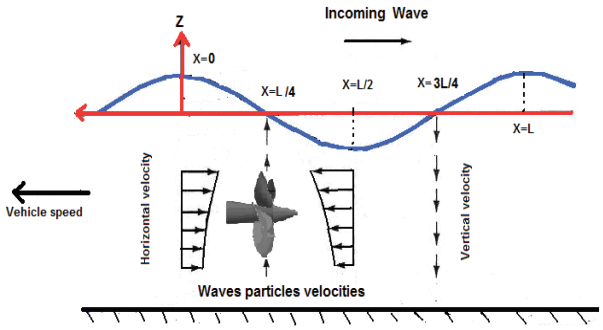

Figure 13: Wave particles velocities in the propeller plane at different locations

The interaction of the wave induced velocities, the velocities induced by the hull motion, and the steady wake field creates a complex velocity field which we know will not be homogeneous over the propeller, and thereby will create side forces and bending moments.

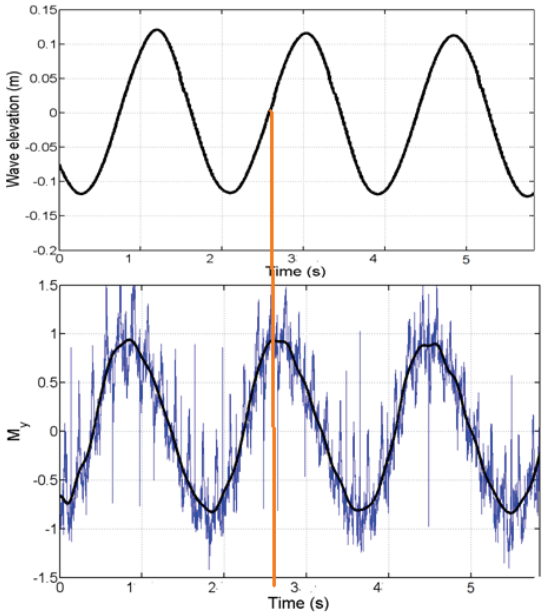

Figure 14: Variation of the loads on the propeller in open water condition

With a view to the practical use of the results obtained in waves in the strength and vibration of the propeller-shaft system, the results are summarized in Figure 15 to Figure 20.

The loads are presented as the ratio between the max values found in waves and the mean load with no waves for different advance velocities and wave amplitudes. It is seen that the bending load fluctuation increases with the increase in the wave amplitude. The bending load fluctuation is larger for the head sea condition compared with the following sea for the particular wave condition being tested. (In following seas, it is normally required to apply higher azimuth angles to keep a straight course compared to the head sea condition. In this study, the effect of higher azimuth angles in following seas will of course not appear since the thrusters are fixed.)

The amplitudes are made non-dimensional by the obtained behind the hull in calm water. The results show that the forces and moments increase considerably due to waves and ship motion.

Figure 21-Figure 26 show the propeller loads in waves divided by the ratio of the wave amplitude to the propeller diameter in order to present the results as a kind of transfer function.

The results obtained for the loads in waves are summarized as below:

1. The load fluctuation increased with an increase in the wave amplitude.

2. The trend is more pronounced in the head sea condition, with the load component amplitude reaching large values compared with those in calm water with no ship motion.
3. In the following sea case, the force fluctuations do not depend strongly on the wave amplitude.
4. Thrust and torque fluctuations do not show a strong dependency on the sea state

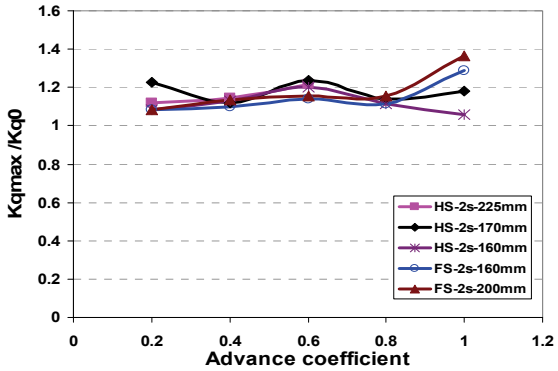

Figure 15: Amplitude of torque on the propeller in waves, as the ratio of the values to those in calm water

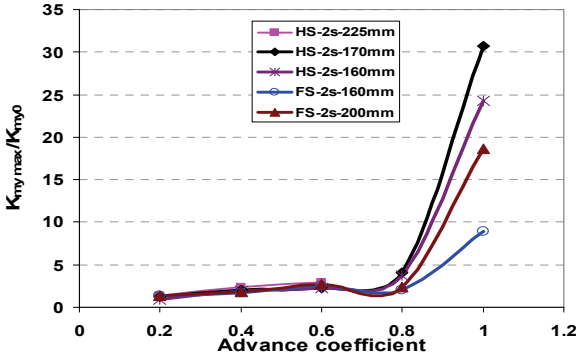

Figure 16: Amplitude of horizontal component of moment on the propeller in waves, as the ratio of the values to those in calm water.

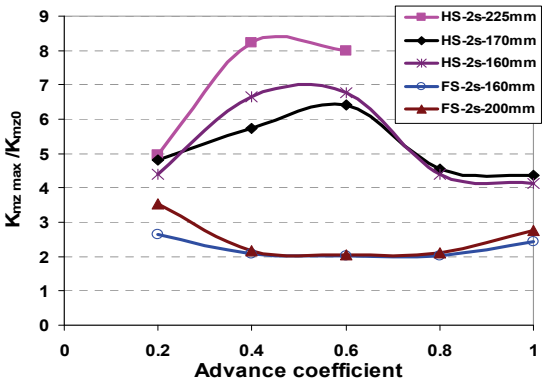

Figure 17: Amplitude of vertical component of moments on the propeller in waves, as the ratio of the values to those in calm water

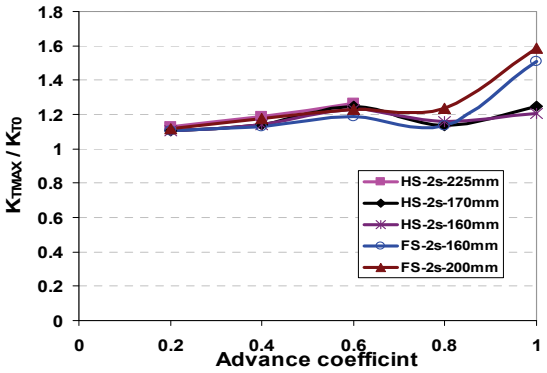

Figure 18: Amplitude of thrust on the propeller in waves , as the ratio of the values to those in calm water

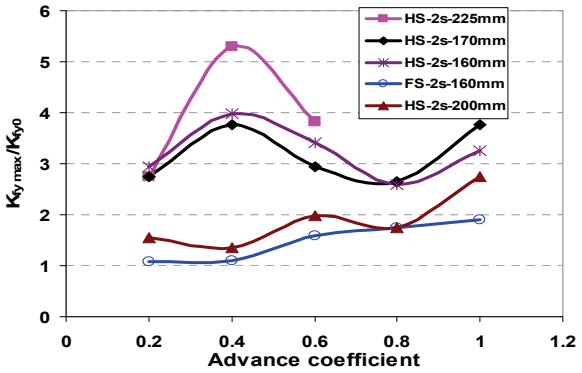

Figure 19: Amplitude of horizontal components of force on the propeller in waves , as the ratio of the values to those in calm water

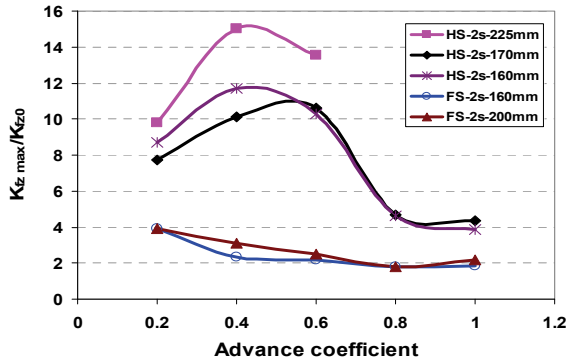

Figure 20: Amplitude of vertical components of force on the propeller in waves , as the ratio of the values to those in calm water

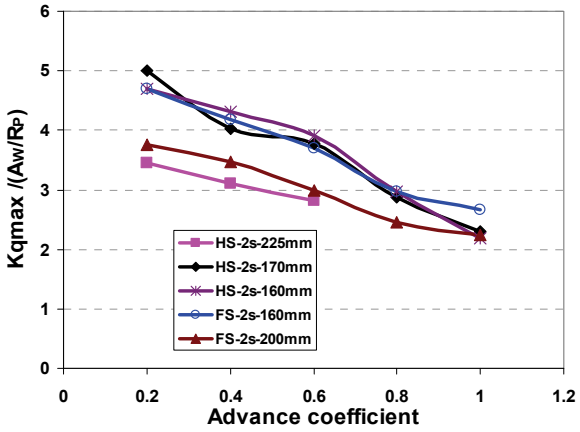

Figure 21: Amplitude of torque on the propeller in waves

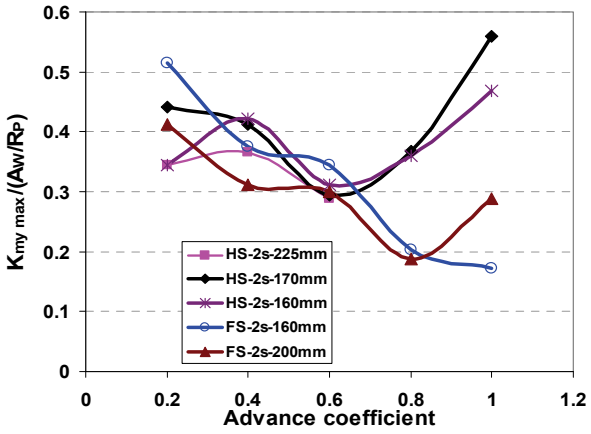

Figure 22: Amplitude of horizontal component of the moments on the propeller in waves

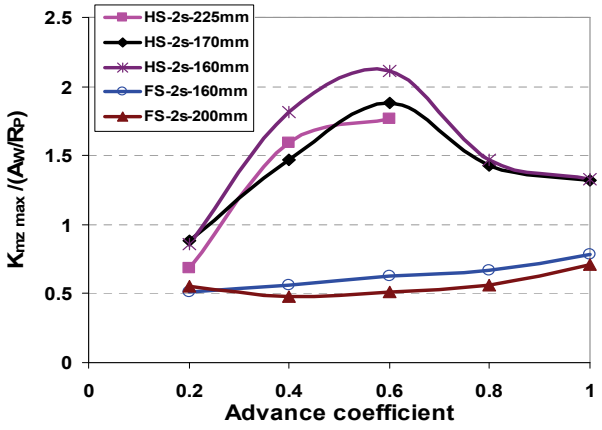

Figure 23: Amplitude of vertical component of the moment on the propeller in waves

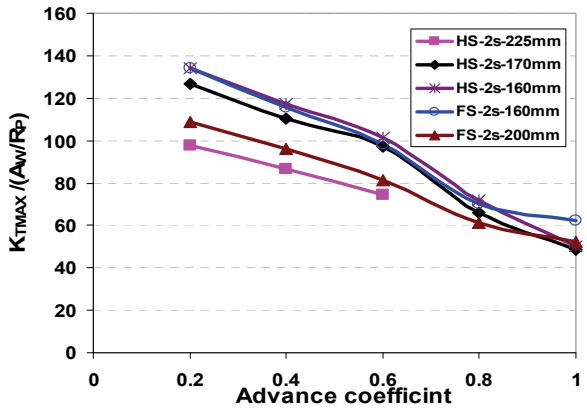

Figure 24: Amplitude of thrust on the propeller in waves

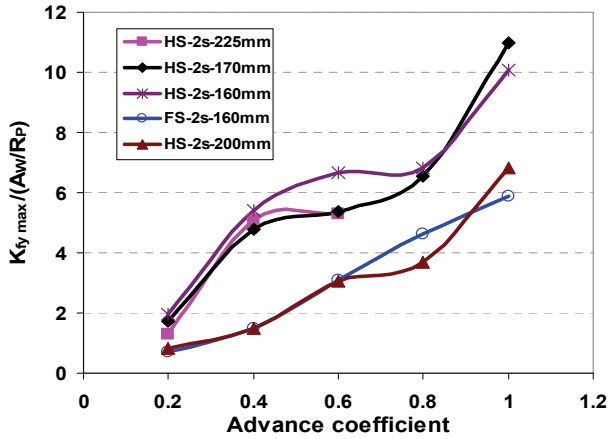

Figure 25: Amplitude of horizontal components of force on the propeller in waves

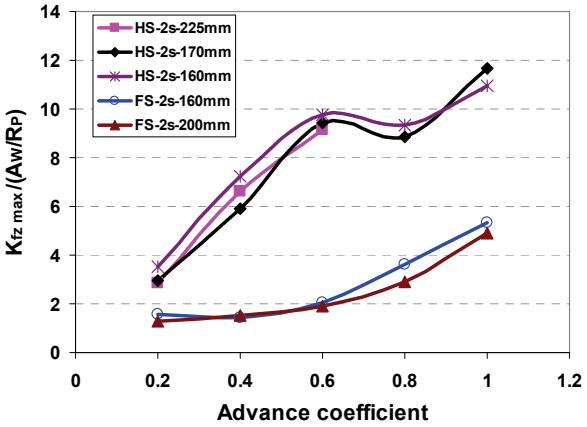

Figure 26: Amplitude of vertical component of the force on the propeller in waves

4. MAXIMUM DESIGN LOADS FOR THE MECHANICAL COMPONENT

The same approach used in reference [2] is implemented to show the importance of the hydrodynamic lateral force and bending moment for the design of shaft bearings.

The loads at the bearings' position are estimated both with and without considering the hydrodynamic loads in waves and in oblique flow.

Common practice when designing bearings for the propeller shaft is recommended by shaft specialists that the resultant vertical force including an equivalent force converted from the bending moment at the propeller centre should be maintained approximately less than 50% of the propeller weight upward in the opposite direction of the propeller weight (Molland.et al., ITTC. 2005). In Figure 27, a typical arrangement of the shaft bearings used for an azimuth thruster is shown. Based on this layout, the contribution of the propeller weight on the bearing can be found:

At bearing C = $-2W_p$ in z direction

At bearing A = W_p in z direction

When the thruster operates at large azimuth angles or in waves, there will be significant side forces and bending moments induced on the shaft by the propeller. These hydrodynamic imposed forces and moments will contribute to the bearing loads in addition to the propeller weight. Thus, the total bearing forces can be evaluated by converting the vertical and horizontal hydrodynamic lateral forces and bending moments on the propeller to forces on the bearings.

Expressions for the resulting total bearing forces F_z^* and F_y^* at **A** and **C** are given below.

At bearing **A**:

$$F_z^* = \left[f_z + \frac{m_y}{0.3D_p} \right] + W_p, \; F_y^* = \left[f_y - \frac{m_z}{0.3D_p} \right] \quad (1)$$

And at bearing C:

$$F_z^* = -\left[2f_z + \frac{m_y}{0.3D_p} \right] - 2W_p, F_y^* = -\left[2f_y - \frac{m_z}{0.3D_p} \right] \quad (2)$$

And the radial force at A and C:

$$Fr^* = \sqrt{F_z^{*2} + F_y^{*2}} \quad (3)$$

D_p is the propeller diameter, m_y and m_z are hydrodynamic imposed moments around the y and z-axes respectively, and f_y and f_z are hydrodynamic imposed lateral and vertical forces on the propeller. Note that we have assumed that the bearing at **C** takes only the radial forces and the bearing at **A** takes only radial and axial forces – the bearings don't take bending moments.

From Figure 28 and Figure 29, it is found that the total bearing loads including hydrodynamic side forces and bending moments for high advance coefficients and heading angles are three times higher for bearing C and four times higher for bearing A compared to the consideration of only the propeller weight in the design of the bearings. The loads in positive heading angles are bigger than in negative heading angles for both open water and behind conditions.

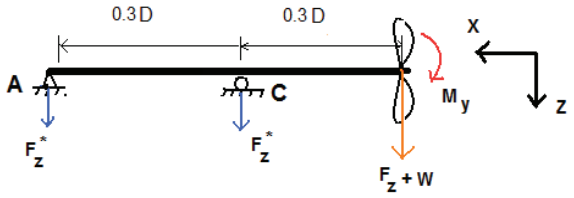

Figure 27: Layout of the propeller shaft bearings and hydrodynamic force and moment of a typical azimuth thruster

Again from Figure 30 and Figure 31, it is found that bearing loads including hydrodynamic forces in waves are two times higher for bearing C and three times higher for bearing A than when we consider only the propeller weight in the design of the bearings.

Therefore, it is seen that the bearing loads are critical even for low advance coefficients and small heading angles.

Hydrodynamic imposed bearing loads may also be important for the stern tube bearings in conventionally shafted propellers, since this system will also experience significant side forces and bending moments caused by waves and oblique flow when the rudder-propeller system operates in a turning situation. The type of stern tube bearings used for conventionally shafted propellers is especially sensitive to the propeller shaft having an angle relative to the straight, undisturbed shaft direction. Even though the magnitude of the bearing loads in waves is relatively smaller than in high oblique inflow, the high number of load cycles experienced by operation in waves may cause fatigue problems.

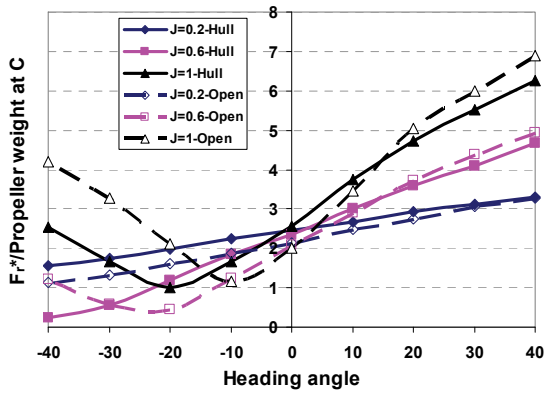

Figure 28: Radial bearing loads in different oblique inflows as a portion of the propeller weight on bearing C (Pulling mode)

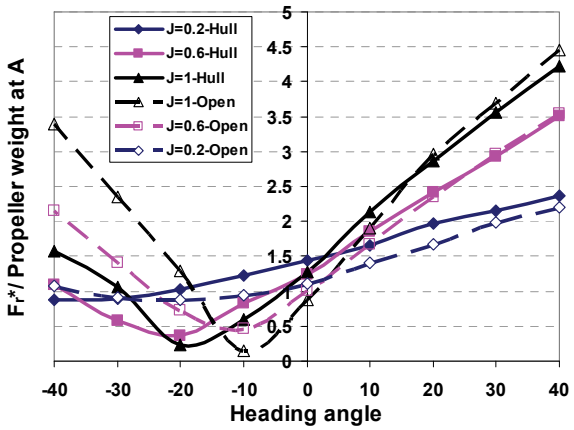

Figure 29: Radial bearing loads in different oblique inflows as a portion of the propeller weight on bearing A (Pulling mode)

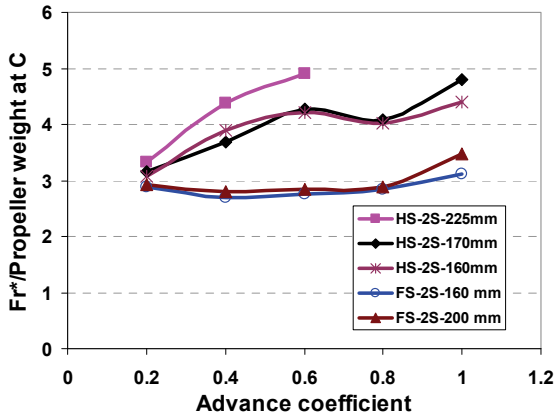

Figure 30: Amplitude of radial bearing loads in waves as a portion of the propeller weight on bearing C (Pulling mode)

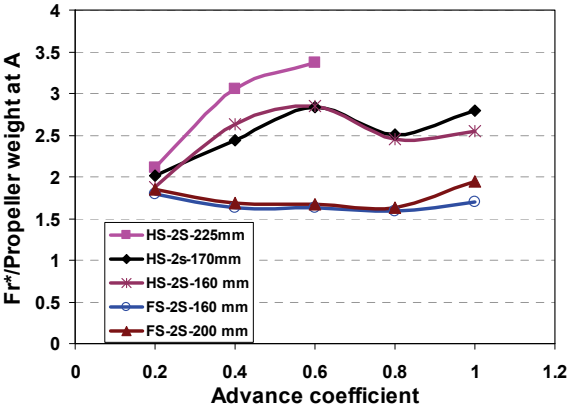

Figure 31: Amplitude of radial bearing loads in waves as a portion of the propeller weight on bearing A (Pulling mode)

5. CONCLUSIONS

It is found that the hydrodynamic side force and bending moment are quite large in both oblique inflow and in waves – significantly larger than the design values suggested by ITTC. Larger side forces and bending moments are found at high azimuth angles in calm sea than in waves (propeller azimuth angle was fixed at zero in waves), although extreme wave conditions were not tested.

Regarding the ship hull wake influence on the propeller loads in different azimuth angles, it is found that the hull wake has a strong effect on the propeller performance and shaft bending loads when propeller is turned outwards from the ship hull centreline. Then the propeller experiences much lower loads in the vicinity of the hull wake compared to the open water condition - while only a small difference is seen in forces and moments between inward heading angles in the behind and open water conditions. The maximum side forces and bending moments experienced in calm water behind the hull are of the same order of magnitude as in open water. However, different hull shapes might give different results in this respect.

The side force and bending moment in waves are considerably larger than in calm water at zero azimuth angle. The propeller experiences larger bending loads in the head sea than in following sea condition (It is also a limited number of wave cases that has been tested (wave period was kept constant).

Finally, hydrodynamic side forces and bending moments are important for both steerable thrusters and shafted propeller systems, and should be considered in the design of propulsion drive train and its mechanical components. Even though a shafted propeller system operates less in highly oblique flow compared to an azimuth propulsor, the propeller will experience significant side forces and bending moments in waves.

6. ACKNOWLEDGEMENTS

This research is sponsored by The Research Council of Norway through the research project SeaPro at The University Technology Centre of Rolls Royce at NTNU.

7. REFERENCES

1. Carlton, J.S., “Marine propeller and propulsion’’, Butterworth Heinemann, Oxford, second edition 2007

2. Amini, H., Steen, S., Spence, S.J. “Shaft side force and bending moment on steerable thrusters in off-design condition’’.11th international symposium on practical design of ships and

other floating structures (PRADS 2010) , Rio de janeiro, Brazil, (2010),

3. Carlton, J. S. "Podded Propulsors: some design and service experience". The Motor Ship Marine Propulsion Conference. Copenhagen, Denmark, April 9-10, 7p. (2002).

4. Molland Anthony, Kim Ki-Han, et.al (2005).Report of the propulsion committee. Proceedings of the 24th ITTC-Volume I, UK

5. Vartdal Bjørn John. et.al. "Lateral Propeller Forces and their Effects on Shaft Bearings''. First International Symposium on Marine Propulsors smp'09, Trondheim, Norway. (2009)

6. Stettler, J.W., "Steady and Unsteady Dynamics of an Azimuthing Podded Propulsor Related to Vehicle Manoeuvring", PhD Dissertation, Massachusetts Institute of Technology. 2004.

7. Minsaa, K.J. and Lehn, E. "Hydrodynamical characteristics of rotatable thrusters", NSFI report R-69.78, The Ship Research Institute of Norway, Trondheim, Norway, (1978).

8. Islam, M.F., Veitch, B., Akinturk, A., Bose, N. and Liu, P., "Experiments with Podded Propulsors in Static Azimuthing Conditions". 8th CMHSC, St John's, NL, Canada. 2007a.

9. Islam, M.F., Veitch, B., Akinturk, A. Bose, N. and Liu, P. 2009. "Performance study of podded propulsors in static azimuthing conditions". International Shipbuilding Progress, 56(3-4): 135-157.

10. Islam, M.F., Akinturk, A., Veitch, B. and Liu, P. "Performance characteristics of static and dynamic azimuthing podded propulsors". Proceedings, International Symposium on Marine Propellers, Trondheim, 2009.

11. Liu, P., Islam, M.F., and Veitch, B. "Unsteady hydromechanics of a steering podded propeller unit". Ocean Engineering, 36(12-13): 1003-1014. 2009.

12. Ball, W.E., Carlton, J.S. "Podded propulsor shaft loads from free – running model experiments in calm water and waves". J. Maritime Eng., Trans RINA.148, (Part A4), 2006.

13. Koushan Kourosh, Spence Silas J.B. Experimental investigation of the Effect of Wave and Ventilation on Thruster Loadings. First International Symposium on Marine Propulsors SMP'09, Trondheim, Norway, (2009).

14. Sampson, R., "Resistance and Propulsion". Lecture note MAR 2010, School of Marine Science and Technology, Newcastle University, UK. February 2008a